JOC*Article*

Stable Simple Enols. Resolution of Chiral 1-[9′-(2′-Fluoroanthryl)]-2,2-Dimesitylethenol. A Different Racemization Mechanism for the Enol and its Acetate[1]

Elimelech Rochlin and Zvi Rappoport*

Department of Organic Chemistry, The Hebrew University, Jerusalem 91904, Israel

zr@vms.huji.ac.il

Received July 29, 2002

Chiral 1-[9′-(2′-methoxyanthryl)]-2,2-dimesitylethenol (**2**), 1-[9′-(2′-fluoroanthryl)]-2,2-dimesitylethenol (**3**), and 1-[9′-(2′-fluoroanthryl)]-2,2- dimesitylvinyl acetate (**4**) were synthesized and their DNMR behavior in $C_6D_5NO_2$ was studied. **3** and **4** were resolved on an amylose tris(3,5-dimethylphenylcarbamate) HPLC column to their enantiomers. Acetate **4** racemizes slowly in solution with $\Delta G_e^{\ddagger}$, $\Delta H_e^{\ddagger}$, and $\Delta S_e^{\ddagger}$ values of 26.2, 27.6 kcal mol^{-1}, and 4.3 eu, respectively, as expected for a rotational $\beta\beta'$-2-ring flip process in a vinyl propeller and the racemization is unaffected by added TFA, Et_3N, and EtOD. Although **3** racemizes almost 350 times faster, the racemization is catalyzed by TFA and shows bell-shape catalysis by Et_3N and a KIE in a partially deuteriated solvent. From this and the DNMR data, it is concluded that **3** does not racemize via a rotational $\beta\beta'$-2-ring flip. Five nonflip routes are discussed for the racemization of **3**, and it is concluded that only the one initiated by protonation at C1 does not contradict the experimental data. By analogy with the E/Z isomerization of the structurally related 2-(*m*-methoxymesityl)-1,2-dimesitylethenol **17**, it is suggested that in the absence of added catalyst one or more enol molecule(s) catalyze the enantiomerization of another one. Only partial resolution was achieved for **2** and from the similarity of its behavior with that of **3**, it is suggested that it racemizes by the same mechanism.

Introduction

The static and dynamic stereochemistry of crowded atropisomeric triarylvinyl systems, e.g., **1** (Mes = mesityl) were investigated during the last two decades. The following features are relevant to their racemization mechanism: (i) They have a chiral propeller conformation in both the solid state and in solution.[2] (ii) Their stereoisomerizations were analyzed in terms of flip mechanisms[3] postulated by Kurland et al.[4a] and analyzed in detail by Mislow et al.[4b] In such correlated rotational processes, the flipping ring passes through a plane perpendicular to the reference double bond plane, whereas the other rings concurrently disrotate and pass through the reference plane. Depending on the number of flipping rings during the rotation the mechanisms are designated as zero-, one-, two-, or three-ring flips. The idealized transition states for the 3-ring flip and the three different 2-ring flip processes are shown in Figure 1. 1-Ring flips are excluded due to their calculated very high energies.[5] The threshold mechanism for helicity reversal in most crowded triarylvinyl propellers is the 3-ring flip with activation barriers of 15−19 kcal mol^{-1}.[2,3]

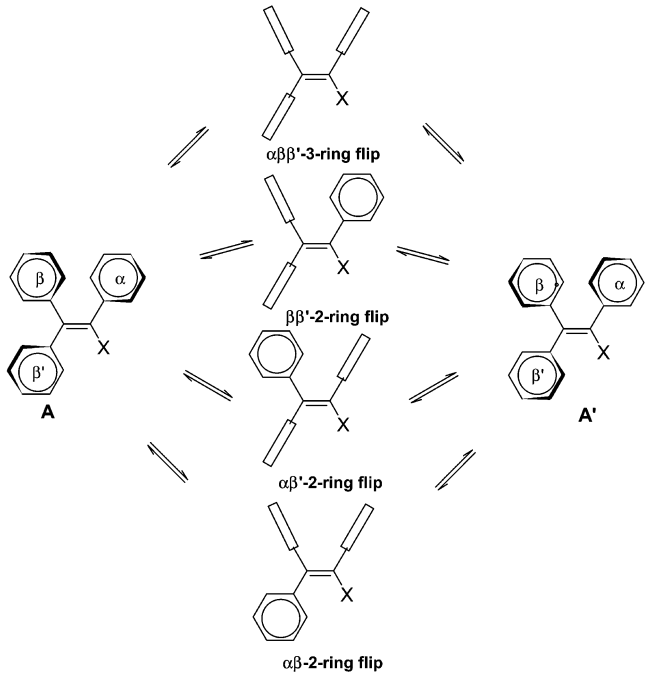

FIGURE 1. Three-ring flip and three different two-ring flips in a three-bladed vinyl propeller. For the transition states, rectangles designate a ring perpendicular to the C=C plane. Phenyl rings rather than bulkier aryls are drawn in order to simplify the structures.

(iii) 2-Ring flip mechanisms (Figure 1) with higher barriers of 21−27 kcal mol^{-1} were also observed. They

(1) Presented in part in the 13th IUPAC Conference on Physical Organic Chemistry, Seoul, Korea, August 25−29, 1996; Rappoport, Z.; Frey, Y.; Sigalov, M.; Rochlin, E. *Pure Appl. Chem*. **1997**, *69*, 1933.
(2) Biali, S. E.; Rappoport, Z. *Acc. Chem. Res*. **1997**, *30*, 307.
(3) Biali, S. E.; Rappoport, Z. *J. Am. Chem. Soc*. **1984**, *106*, 477.
(4) (a) Kurland, R. J.; Schuster, I. I.; Colter, A. K. *J. Am. Chem. Soc*. **1965**, *87*, 2279. (b) Mislow, K.; Gust, D.; Finocchiaro, P.; Boettcher, R. J. In *Topics in Current Chemistry*, No. 47, Stereochemistry 1; Springer-Verlag: Berlin, 1974; p.1.
(5) Rochlin, E.; Rappoport, Z. *J. Org. Chem*. **1994**, *59*, 3857.

10.1021/jo020497q CCC: $25.00
Published on Web 12/14/2002

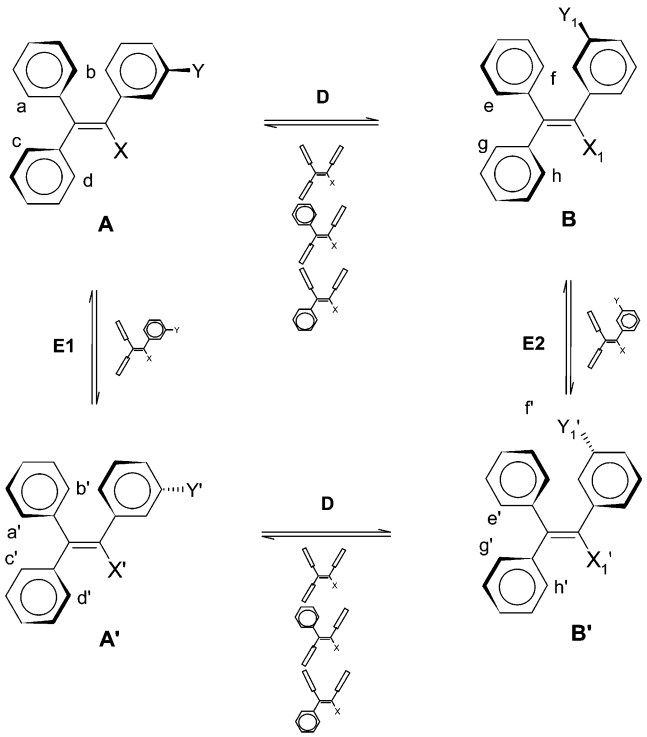

FIGURE 2. Four stereoisomers and their interconversions in a singly labeled vinyl propeller, demonstrated for a *m*-Y-substituted α-ring. Transition states are below or on the side of the arrows.

were monitored by DNMR or by resolution followed by racemization of systems in which one ring was labeled in turn with a *m*-OMe group and the results were corroborated by force field calculations.[5] The "unlabeled" system with local C_{2v} symmetry of all the three rings, exists as a pair of enantiomers A and A′ (Figure 1). The threshold 3-ring flip process exchanges the edges of the rings and interconverts the two enantiomers. Hence, higher energy flip processes will be unobservable either by racemization of a resolved "vinyl propeller" or by DNMR studies. Labeling one edge in any of the rings by a group Y creates two pairs of enantiomers A and A′ and B and B′ (Figure 2). The 3-ring flip process then results in diastereomerization D (A⇌B and A′⇌B′ interconversion) whereas the enantiomerizations E1 and E2 (A⇌A′ and B⇌B′ interconversions, respectively) require a 2-ring flip with an unflipping labeled ring. This process can be directly observed either by resolution of enantiomers and monitoring their racemization or by DNMR. If Y has minor steric or electronic effects, the labeled system can serve as a model for the "invisible" 2-ring flips in the unlabeled molecule. It was shown that *m*-OMe substitution does not affect much the geometry and rotational barriers in $Mes_2C{=}C(X)Mes$ systems. Thus, the 3-ring flip and the three different 2-ring flip routes were studied for X = H,[6] X = OAc[7,8] and X = OPr-*i*.[5] The relative order of the barriers of the four different flip processes was found to strongly depend on X.

(6) Biali, S. E.; Rappoport, Z. *J. Org. Chem*. **1986**, *51*, 2245.
(7) Biali, S. E.; Rappoport, Z.; Mannschreck, A.; Pustet, N. *Angew. Chem., Int. Ed. Engl.* **1989**, *28*, 199.
(8) Rochlin, E.; Rappoport, Z.; Kastner, F.; Pustet, N.; Mannschreck, A. *J. Org. Chem*. **1999**, *64*, 8840.

TABLE 1. Sites Exchanged for the Four Flip Mechanisms in α-ring Labeled Triarylvinyl Propeller

mechanism	isomerization process	resulting site exchanges[a]
αββ′-3-ring flip	D: A ⇌ B	(af)(be)(ch)(dg)(XX_1)(YY_1)
	A′ ⇌ B′	(a′f′)(b′e′)(c′h′)(d′g′)(X′X_1′)(Y′Y_1′)
αβ′-2-ring flip	D: A ⇌ B	[(ae)(bf)](ch)(dg)(XX_1)(YY_1)
	A′ ⇌ B′	[(a′e′)(b′f′)](c′h′)(d′g′)(X′X_1′)(Y′Y_1′)
αβ-2-ring flip	D: A ⇌ B	(af)(be)[(cg)(dh)](XX_1)(YY_1)
	A′ ⇌ B′	(a′f′)(b′e′)[(c′g′)(d′h′)](X′X_1′)(Y′Y_1′)
ββ′-2-ring flip	E1[b]: A ⇌ A′	(ab′)(ba′)(cd′)(dc′)(XX′)(YY′)
	E2[b]: B ⇌ B′	(ef′)(fe′)(gh′)(hg′)(X_1X_1′)(Y_1Y_1′)

[a] Square brackets mean that superposition of two processes, i.e., the specified 2-ring flip and a much faster 3-ring flip, takes place, which resulted in additional exchange between the four sites in the nonflipping ring. [b] These two diastereomeric enantiomerization processes are experimentally indistinguishable due to averaging of the signals of diastereomers by a fast 3-ring flip process.

(iv) For crowded stable enols, i.e., **1**, X = OH only the threshold 3-ring flip was investigated[3] because an obstacle was met on attempted study of the 2-ring flip processes. Labeling of either the *β*- or the *β*′-Mes ring gave both E and Z isomers that readily mutually interconvert, resulting in a mixture of 4 pairs of enantiomers (2 pairs for each geometric isomer), which is difficult to analyze or separate.[5,9] Such an easy "spontaneous" noncatalyzed E/Z-isomerization in solution was not observed for **1**, X ≠ OH and it is unique for enols. The isomerization rate is comparable to those for the 2-ring flip processes mentioned above.[9] Although labeling of both *β*-mesityl rings with an identical tag eliminates the E/Z-isomerism, a mixture of 4 pairs of enantiomers is still formed.[3,9]

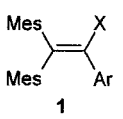

1

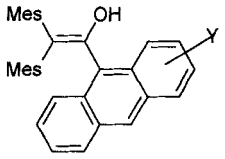

1a

There is an alternative to make all the three 2-ring flips observable, while labeling only the α-aryl ring. Figure 2 demonstrates isomerization processes and Table 1 analyses the site exchanges accompanying the different flip mechanisms. The diastereomerization D may result from either the αββ′-3-ring, the αβ-2-ring, or the αβ′-2-ring flip process, when the 3-ring flip is the lower energy pathway [3]. *The diastereomeric E1 and E2 enantiomerization routes may proceed via the ββ′-2-ring flip* (Table 1, Figure 2). It is seen from Table 1 that the *αβ- and αβ′-2-ring flip processes exchange the edges of the β′ and the β rings, respectively, whereas the ββ′-2-ring flip exchanges the edges of both rings in a single process.* Consequently, if the ββ′-2-ring flip is the lowest energy 2-ring flip, the other 2-ring flips will be unobservable. Edges exchange in the *β*′ and *β* rings will have an activation barrier identical to that for the enantiomerization process. In contrast, if the ββ′-2-ring flip is the highest energy 2-ring flip, the αβ- and αβ′-2-ring flips will be observable and edges exchange in the *β*′ and *β* rings will have different barriers which are lower than that for the enantiomer-

(9) Rochlin, E.; Rappoport, Z. *J. Org. Chem*., in press.

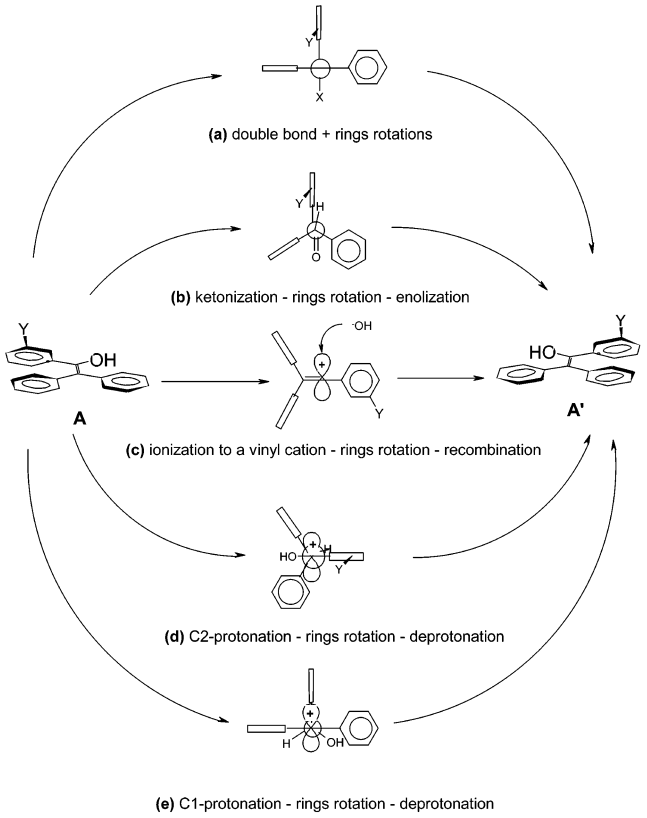

FIGURE 3. Five possible nonflip routes for the enantiomerization in a singly labeled vinyl propeller.

ization. Such a situation will be favored when the α-ring will be bulkier when in plane than the *β*- and *β*′-rings, as e.g., in enol **1a** with a substituted α-9-anthryl ring and two *β*- and *β*′-Mes rings.

(v) Contribution of nonflip routes was previously excluded concerning the threshold 3-ring flip process in 1,2,2-trimesitylethenol.[3] We apply the term "nonflip"[3] to five routes: (a) rotation around the double bond, (b) ketonization−rotation−re-enolization, (c) C1−O bond ionization to a vinyl cation − rings rotation−cation + leaving group recombination, (d) and (e) proton addition to C1 or C2 of the double bond−rotation−proton elimination (Figure 3). They should not be a priori excluded when discussing the higher energy 2-ring flips.

(vi) Attempts to resolve the enantiomeric pairs of unlabeled systems **1** with three rings possessing local C_{2v} symmetry had failed [3], due to the low 3-ring flip enantiomerization barriers. However, enantiomerization of labeled systems where only one ring possesses a lower C_s symmetry proceeds via a higher barrier 2-ring flip (Figure 2) and several such systems were successfully resolved.[7,8] However, chiral enols **1**, X = OH were never resolved.

Several questions emerge from these data. (1) Do crowded labeled triarylethenols racemize via the 2-ring flip route as when X ≠ OH or via a "nonflip" route? (2) In the former case, could we observe all the three 2-ring flip processes? (3) What is the mechanism in the latter case? (4) Could we resolve these crowded enols to their enantiomers?

To answer these questions, we synthesized the 1-[9′-(2′-substituted anthryl)] ethenols **2** and **3** and an acetate

SCHEME 1. Synthesis of 2−4

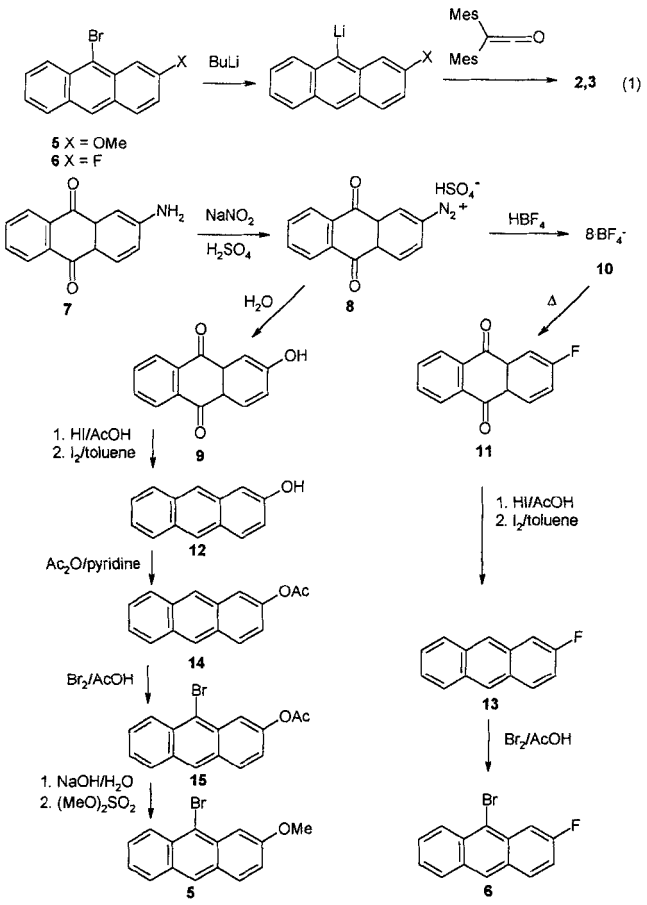

4 and attempted to follow their DNMR behavior and to resolve them and study their subsequent racemization.

Results and Discussion

Synthesis. Enols **2** and **3** were synthesized by reacting dimesitylketene[10] with a 2-substituted 9-anthryllithium reagents. The latter were prepared in situ by lithiation of 2-substituted 9-bromoanthracenes **5** and **6** (eq 1) which were synthesized in turn from the commercially available 2-aminoanthraquinone **7** by the sequence shown in Scheme 1. **7** was diazotized in concentrated H_2SO_4 and the diazonium salt **8** was hydrolyzed to 2-hydroxyanthraquinone **9**. Alternatively, the diazonium tetrafluoroborate **10** was isolated and thermally decomposed to 2-fluoroanthraquinone **11**. When the anthraquinones **9** and **11** were reduced to the anthracenes **12** and **13** by hydroboration with $NaBH_4/BF_3$ in diglyme[11] the yields of the desired anthracenes were ⩽ 35% due to formation of the byproducts 2-substituted anthrones and 9,10-dihydroxy-9,10-dihydroanthracenes. Reduction with HI in AcOH at ca. 120 °C was more effective and gave a mixture of the desired anthracene and up to 40% of the 9,10-dihydro derivative, which on treatment with iodine afforded the anthracene in 80−90% yield. Careful bromination of 2-fluoroanthracene **13** afforded a good yield

(10) Fuson, R. C.; Armstrong, L. J.; Chadwick, D. H.; Kneisley, J. W.; Rowland, S. P.; Shenk, W. J.; Soper, Q. F. *J. Am. Chem. Soc.* **1945**, *67*, 386.

(11) Bapat, D. S.; Subba Rao, B. C.; Unni, M. K.; Venkataraman, K. *Tetrahedron Lett.* **1960**, 15.

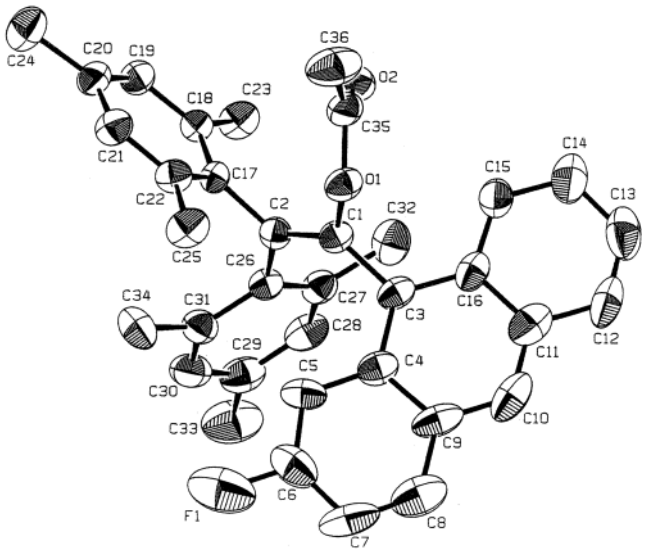

FIGURE 4. ORTEP drawing of the X-ray structure of **4**.

TABLE 2. Selected Crystallographic Data for 4 and 16 (designations according to Figure 4)

parameter	**4**	**16**[13]
bond length, Å		
C1−C2	1.346	1.339
C1−C3	1.492	1.477
C1−O1	1.428	1.382
C2−C26	1.511	1.500
C2−C17	1.508	1.507
bond angle, deg		
C1C2C26 (α_1)	121.1	121.2
C17C2C26 (α_2)	117.1	118.5
C1C2C17 (α_3)	121.8	120.2
C2C1C3 (α_4)	130.7	128.0
C3C1O1 (α_5)	110.3	113.3
C2C1O1 (α_6)	118.6	118.8
torsional angle, deg		
Ant/C=C plane (φ_α)	65.5	62.5
β-Mes/C=C (φ_β)	55.9	58.2
β'-Mes/C=C($\varphi_{\beta'}$)	58.6	56.9
C3C1O1/C17C2C26(θ)	7.2	−2.1

(70%) of 9-bromo-2-fluoroanthracene **6**, accompanied by a small amount of the 9,10-dibromo derivative.

2-Hydroxyanthracene **12** could not be selectively brominated at C-9 or C-10.[12] It was therefore first acetylated to 2-acetoxyanthracene **14** which was brominated to 9-bromo-2-acetoxyanthracene **15**, analogously to **13**. In a one-pot procedure, **15** was hydrolyzed and the product was O-methylated to the 9-bromo-2-methoxyanthracene **5**. The location of the bromine at C-9 of **5** and **6** was established unequivocally by their COSY and NOESY ^{1}H NMR spectra. E.g., in **5** there is only a single one-proton singlet at 8.32 ppm that belongs to one of the "meso" 9 and 10 positions. This proton and the H_4 doublet (^3J = 9.1 Hz) at 7.86 ppm show a strong NOE correlation, whereas a NOE correlation with the H_1 doublet (^4J = 2.3 Hz) at 7.66 ppm is absent. This assign the proton as H_{10} and hence the 9-position is occupied by bromine.

The enol acetate **4** was prepared by acetylation of **3** and its solid-state structure was established by X-ray diffraction.

(12) Yoffe, I. S.; Efros, L. S.; Sheglova, Z. N. *Z. Obshch. Chim*. **1936**, *9*, 1128.

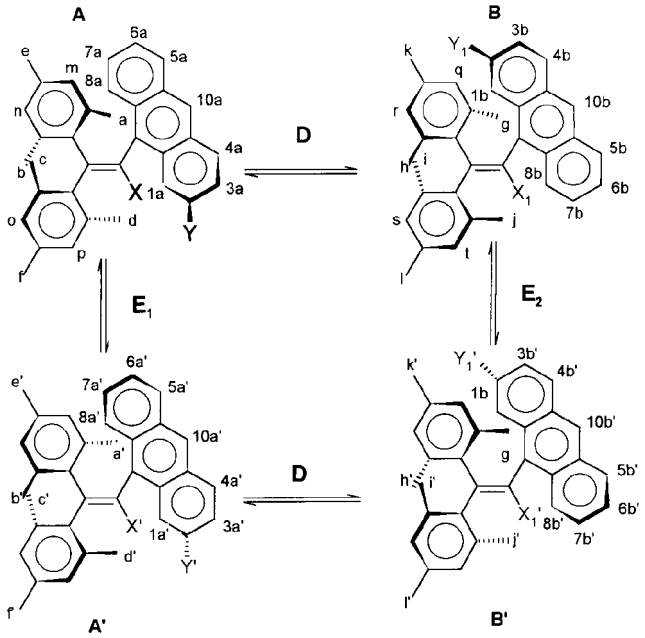

FIGURE 5. Four stereoisomers and their interconversion ring-flip routes in **2**,**3** and **4**.

Crystal Structure of 4. X-ray structure of **4** (ORTEP in Figure 4, and stereoview, crystallographic data, bond lengths and angles, positional and thermal parameters are in Figure S1 and Tables S1−S5 in the Supporting Information) reveal several features, which are compared with those of enol **16**[13] (Table 2). **4** possesses a propeller conformation with torsional angles of the rings α and β' neighboring to the OAc group which are 1.7°−3° larger, and that of the β-ring 2.3° smaller than in **16**. The double bond in **4** is twisted by θ = 7.2°, 5.1° more than in **16**. The analogous angle for 1,2,2-trimesitylvinyl acetate is 10°.[3,13]

Static and Dynamic NMR Study of 2, 3, and 4. The molecules of **2**−**4** should exist in solution as a mixture of two enantiomeric pairs (Figure 5). For a "frozen" propeller

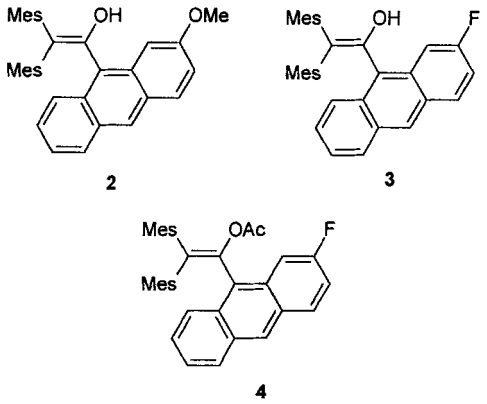

conformation on the NMR time scale and in the absence of signals overlap each diastereotopic proton or group will exhibit a separate signal, i.e., 12 Me and 8 H mesityl (Mes-H) rings signals, 16 H anthryl (Ant-H) ring signals and 2 signals each of the anthryl and vinyl substituents

(13) Kaftory, M.; Biali, S. E.; Rappoport, Z. *J. Am. Chem. Soc.* **1985**, *107*, 1701.

TABLE 3. NMR Data for 2, 3, and 4 in $C_6D_5NO_2$ at 284 K (designations according to Figure 5)

assignment	δ, ppm		
	2	**3**	**4**
β-*o*-Me: a, b, g, h	2.23, 1.81, 2.05, 1.66	2.22,1.67, 2.20, 1.67	2.22,1.68,2.22,1.72
β′-*o*-Me: c, d, i, j	3.015,1.98, 2.94, 1.96	2.94,1.94, 2.96, 1.88	2.87,1.98,2.85,2.00
β-*p*-Me: e, k	1.82, 1.78	1.83, 1.78	1.86, 1.80
β′-*p*-Me: f, l	2.15, 2.33	2.29	2.32
β-Mes-H: m, n, q, r	6.57, 6.17, 6.63, 6.20	6.62,6.18, 6.57, 6.14	6.63,6.19,6.60,6.17
β′-Mes-H: o, p, s, t	7.03, 6.60, 7.06, 6.79	7.08,6.78, 7.08, 6.74	7.10,6.76,7.10,6.76
1a, 1b	8.23, 7.50[a]	8.49[e], 8.11[a]	8.40, 8.23
3a, 3b	7.29[b], 6.76[c]	6.92, 7.38	6.93, 7.37
4a, 4b	8.03, 7.62	8.11[a], 7.67[a]	8.11[a], 7.69
5a, 5b	7.69[a], 8.07	8.13[a], 7.72[a]	8.09[a], 7.70
6a, 6b	7.10[c], 7.52[a]	7.56, 7.12	7.53, 7.18
7a, 7b	7.29[d], 7.67[a]	7.69[a], 7.28	7.67, 7.37
8a, 8b	8.56, 8.72	8.81, 8.49[e]	8.73, 8.62
10a, 10b	8.36, 8.38	8.40	8.38
Xa, Xb	OH: 6.57, 6.15	OH: 6.24, 6.28	OAc: 1.87, 1.92
Ya, Yb	OMe: 4.00, 3.92	F: −114.7, −112.7	

[a] Partly overlaps a nitrobenzene signal. [b] Partly overlaps the H_7 signal. [c] Partly overlaps the β′-Mes-H signal. [d] Partly overlaps the H_3 signal. [e] Overlaps the H_8 or H_1 signal.

Y and X. Experimental ^1H and ^{19}F NMR spectra of these molecules in $C_6D_5NO_2$ at 284 K are in accordance with a frozen propeller conformation in solution (Table 3 and Figure 6a). The diastereomeric ratios are 1:1.3 for **2** and **4** and 1:1.2 for **3**. The signals were assigned by a combination of COSY-DQF, NOESY, F-decoupling ^1H NMR and ^{19}F NMR techniques, by comparison with the ^1H NMR spectrum of **16** and by an accurate signals integration. The H_8, OMe and Mes-H signals in the ^1H spectrum at 400 MHz and the fluorine signals in the ^{19}F spectrum at 376 MHz are well separated both from other signals and from each other and enable a convenient DNMR monitoring of the internal rotation processes.

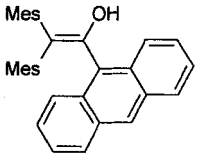

16

E/Z- *m*-MeOMes(Mes)C = C(OH)Mes

17

On raising the temperature, consecutive coalescence processes took place at different temperatures. Those of the H_8, OMe, F, Mes-H, and β′-*o*-Me signals were monitored. All of the 8 pairs of the Ant-H signals of **2**−**4** coalesced, giving a well resolved spectrum of 8 signals at >380 K (Table 4 and Figure 6b). Pairs of OMe signals in the ^1H NMR spectrum of **2** and F signals in the proton-decoupled ^{19}F NMR spectrum of **3** and **4** also coalesce to sharp singlets (Table 4). From the coalescence data (Table 5) for the H_8, OMe, and F signals (sites exchanges [8a,8b] and [Y,Y1] in Figure 5), barriers of $\Delta G_{\alpha\beta\beta'}^{\ddagger} = 15.7$ (for **2**), 16.6 (for **3**), and 16.6 kcal mol^{-1} (for **4**) were calculated (Table 5). These values resemble the threshold αββ′-3-ring flip enantiomerization $\Delta G_{\alpha\beta\beta'}^{\ddagger}$ =16.2 kcal mol^{-1} for the structurally similar 1-(9′-anthryl)-2,2-dimesityl-ethenol **16**[3]. For the Mes-H signals several coalescence processes were observed. The two pairs of the β-Mes-H singlets coalesced first due to a 3-ring flip D process (sites exchanges [mr] and [nq] in Figure 5) and at >380 K a pair of broadened singlets at 6.4−6.5 ppm, belonging to the unexchanged edges of the β-Mes ring, started to rise. These pairs of both **2** and **3** coalesced (sites exchanges [mq] and [nr] in Figure 5) at 413 and 430 K, giving barriers of 21.9 and 22.5 kcal mol^{-1}, respectively (Table 5). Analogously, the two pairs of the β′-Mes-H signals coalesced at >380 K to a one pair at 7.0−7.1 ppm. Then a pair of signals of **3** coalesced at 444.6 K, giving a barrier of 24.6 kcal mol^{-1}, whereas a pair of signals of **2** and two pairs of β- and β′-Mes-H signals of **4** did not interchange at 430−445 K and remained as broad singlets. Likewise, six pairs of Mes-Me signals interchanged gradually. Between 305 and 380 K, three sets of signals, i.e., two pairs of diastereotopic β-*o*-Me and β′-*o*-Me and two *p*-Me signals were observed. The latter remained sharp up to 445 K, whereas the two former pairs of signals broadened and consecutively interchanged. A pair of β-o-Me signals coalesced, whereas a pair of β′-o-Me signals remained as broad separate singlets up to 445 K.

The lower energy process in this cascade exchanges between the pairs of protons and groups of diastereomeric pairs (A⇌B)(A′⇌B′) (Figure 5). It is highly likely that the process followed is a 3-ring flip process (Table 1) as deduced from the similarity of its barrier (Table 5) to that of the closely related **16** [3]. The next higher energy process (Table 5) is due to mixing of only the β-ring signals and the next one is for mixing of only the β′-ring signals. Several flip routes could account for these latter processes. It can be seen from Table 1 that under fast αββ′-3-ring flip process, the αβ′-2-ring flip will exchange only the β-ring sites, whereas the αβ-2-ring flip will exchange only the β′-ring sites. Although the ββ′-2-ring flip process also exchanges diastereotopic sites in β- and β′-rings, the two rings will then exhibit the same barrier, which is clearly not the case. Hence, the following sequence of flip processes fit our data: At low temperatures, the αββ′-3-ring flip interconvert two diastereomers, thus reducing to half the number of signals. At higher temperatures, the αβ′-2-ring flip interchanges the diastereotopic β-ring sites and at much higher temperatures either the αβ- or the ββ′-2-ring flip mixes the diastereotopic sites of the β′-ring. We predict a higher ββ′-2-ring flip barrier than that of the αβ-2-ring flip due to the "in plane" bulk of the anthryl ring.[14] This prediction can be corroborated by monitoring the enantiomerization process, supposedly the ββ′-2-ring flip, by another method independent of the

(14) Hine J.; Skoglurd, M. J. *J. Org. Chem.* **1982**, *47*, 4758.

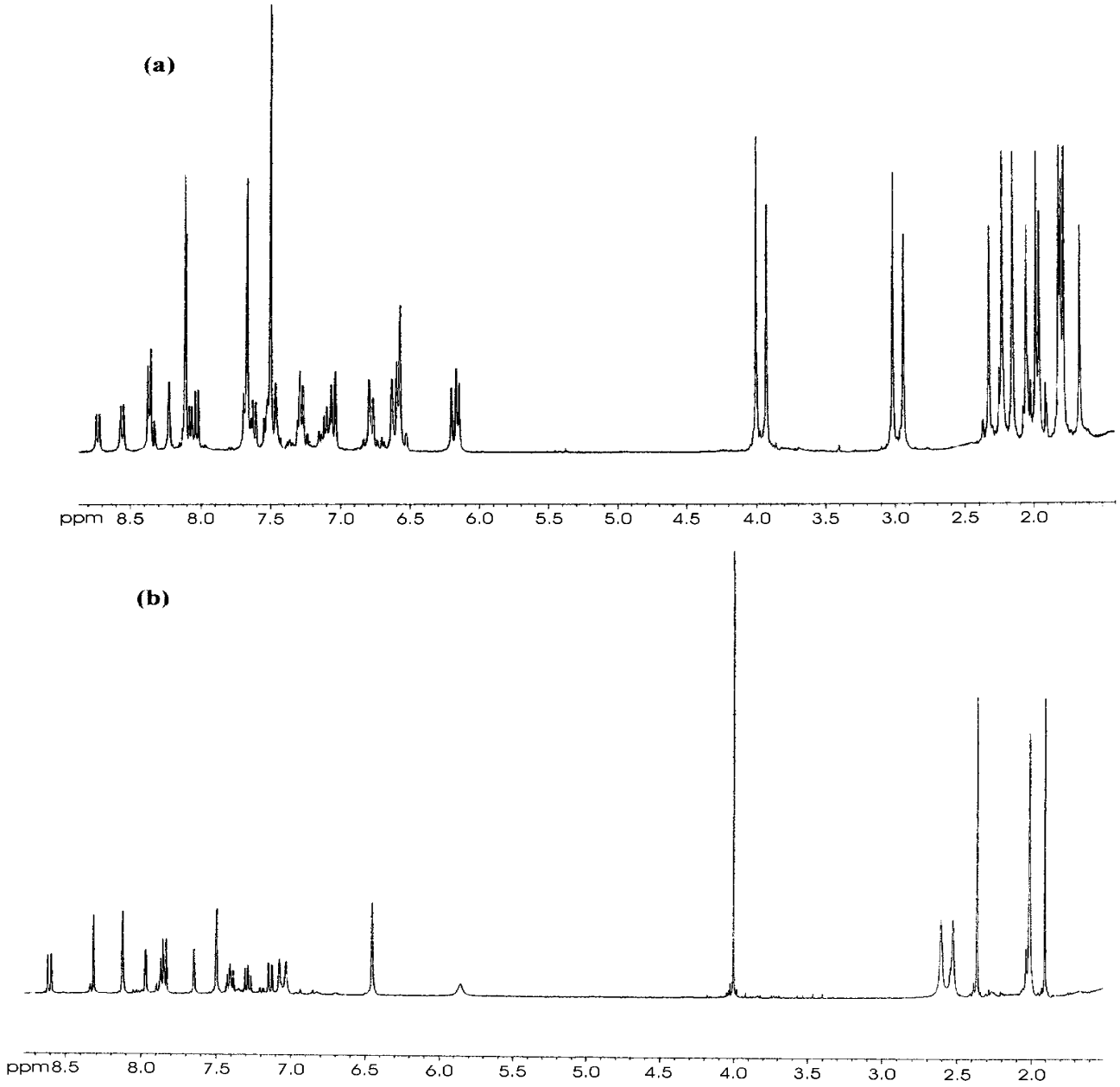

FIGURE 6. ^{1}H NMR spectrum of **2** in $C_6D_5NO_2$: (a) at 284 K (before coalescence), (b) at 430 K (Assignments in Tables 3 and 4).

rings protons. Two approaches are possible. One is to incorporate into the molecule a prochiral NMR probe group, but this will modify the molecule and we have already shown that the order and the magnitude of the barriers are sensitive to steric and electronic effect of the vinyl substituent.[5] An alternative is to resolve the racemic mixture to enantiomers and to monitor the racemization process. We attempted such a resolution of **2**−**4**.

Optical Resolution of 2, 3, and 4. Racemization Experiments. Attempted optical resolution of **2**, **3**, and **4** was performed on a chiral HPLC column (see Experimental Section). Full resolution was achieved for **3** and **4** and only partial resolution for **2**. On attempt to collect sufficient quantities (1−2 mg) of each enantiomer for the racemization experiments we found that whereas both enantiomers of **4** were configurationally stable at room temperature, those of **2** and **3** underwent racemization even at 0 °C. This process was not further investigated for **2**. For **3**, it was monitored by chiral HPLC in 98:1:1 hexane: EtOH: *i*-PrOH at 25.5 °C. A linear plot for the first-order reversible reaction of $\ln(2P_A\text{-}1)$ vs t, where P_A is a molar fraction of the given enantiomer, was obtained from which the racemization and the enantiomerization rate constants $k_{rac} = 1.1 \times 10^{-3}$ s^{-1} and $k_e = 1/2k_{rac} = 5.3 \times 10^{-4}$ s^{-1} were calculated. From k_e, an enantiomerization barrier $\Delta G_e^{\ddagger} = 21.9 \pm 0.1$ kcal mol^{-1} for **3** was derived. *This value is lower than the barrier measured by the coalescence of β′-Mes-H protons (Table 5) and hence is inconsistent with enantiomerization of the enol by the ββ′-2-ring flip route.* This conclusion was further strengthened by a study of the racemization of **4** which was configurationally stable enough to collect 2 mg of each enantiomer and to record their CD spectra. Whereas >2 weeks were required to complete its racemization, that of **3** took <1 h. The racemization of each enantiomer of **4** in 80:20 hexane:*i*-PrOH was studied at 37, 55, and 70

TABLE 4. ^{1}H NMR Data for 2 in $C_6D_5NO_2$ at 430 K

assignment		δ, ppm	multiplicity	^{3}J, ^{4}J, Hz	integration
anthryl ring	H1	7.97	d	2.0	1H
	H3	7.14	dd	9.1, 2.3	1H
	H4	7.84	d	9.1	1H
	H5	7.86	d	8.4	1H
	H6	7.29	m		1H
	H7	7.41	m		1H
	H8	8.61	d	8.9	1H
	H10	8.32	s		1H
β′-Mes-H		7.08	broad s		1H
β′-Mes-H		7.03	broad s		1H
β-Mes-H		6.45	s		2H
OH		5.86	broad s		1H
OMe		4.00	s		3H
β′-*o*-Me		2.60	broad s		3H
β′-*o*-Me		2.52	broad s		3H
β′-*p*-Me		2.36	s		3H
β-*o*-Me		2.01	s		6H
β-*p*-Me		1.90	s		3H

TABLE 5. Coalescence Data for $Mes_2C{=}C(X)AntY$ Derivatives 2, 3, and 4 (designations according to Figure 5)

compd	signal/expected process[a]	Δν, Hz	k_c, s^{-1}	T_c, K	$\Delta G_c^{\ddagger}$, kcal mol^{-1}
2	OMe Y ⇌ Y$_1$ Y′ ⇌ Y$_1$′	24.7	54.9	310.0	15.7 ± 0.1
	Ant-H$_8$ 8a ⇌ 8b 8a′ ⇌ 8b′	64.2	142.7	321.5	15.7 ± 0.1
	β-Mes-H (mr) ⇌ (nq) (m′r′) ⇌ (n′q′)	9.7	21.5	413.0	21.9 ± 0.2
	β′-Mes-H (ot) ⇌ (sp) (o′t′) ⇌ (s′p′)	20.8	46.1	> 430	> 22.2
	β′-*o*-Me (cj) ⇌ (di) (c′j′) ⇌ (d′i′)	24.3	54.0	> 430	> 22.1
3	F Y ⇌ Y$_1$ Y′ ⇌ Y$_1$′	754	1674	376.5	16.6 ± 0.1
	Ant-H$_8$ 8a ⇌ 8b 8a′ ⇌ 8b′	129.3	287.3	346	16.5 ± 0.1
	β-Mes-H (mr) ⇌ (nq) (m′r′) ⇌ (n′q′)	15.4	34.2	430	22.5 ± 0.2
	β′-Mes-H (ot) ⇌ (sp) (o′t′) ⇌ (s′p′)	3.2	7.1	444.6	24.6 ± 0.3
4	Ant-H$_8$ 8a ⇌ 8b 8a′ ⇌ 8b′	45.8	101.7	334.5	16.6 ± 0.1
	β-Mes-H (mr) ⇌ (nq) (m′r′) ⇌ (n′q′)	31.5	70.0	> 445	> 22.6
	β′-Mes-H (ot) ⇌ (sp) (o′t′) ⇌ (s′p′)	17.8	39.5	> 445	> 23.1

[a] Sites which are already mixed by the fast 3-ring flip process, are given in parentheses.

°C. From the first-order linear plots and the linear Arrhenius plot, **4** exhibits high "normal" enantiomerization barrier of $\Delta G_e^{\ddagger}$ = 26.2 kcal mol^{-1} (Table 6) as expected for the ββ′-2-ring flip where in the transition state the α-anthryl ring is in-plane. The low $\Delta S_e^{\ddagger}$ value of 4.3 eu is in line with a monomolecular internal rotation process, which is not accompanied by appreciable changes in charge distribution. Consequently, **4** is likely to enantiomerize by the ββ′-2-ring flip route.

TABLE 6. Kinetic Parameters for the Enantiomerization of 4 in 80:20 Hexane: *i*-PrOH[a]

T, °C	$10^6 k_e$, s^{-1}	$\Delta G_e^{\ddagger}$, kcal mol^{-1}	E_a, kcal mol^{-1}	logA_e	$\Delta H_e^{\ddagger}$, kcal mol^{-1}	$\Delta S_e^{\ddagger}$, e.u.
37	1.8	26.3 ± 0.1	28.3 ± 0.1	14.21	27.6 ± 0.1	4.3
55	24	26.2 ± 0.1				
70	145	26.2 ± 0.1				

[a] $k_{rac} = 2k_e$.

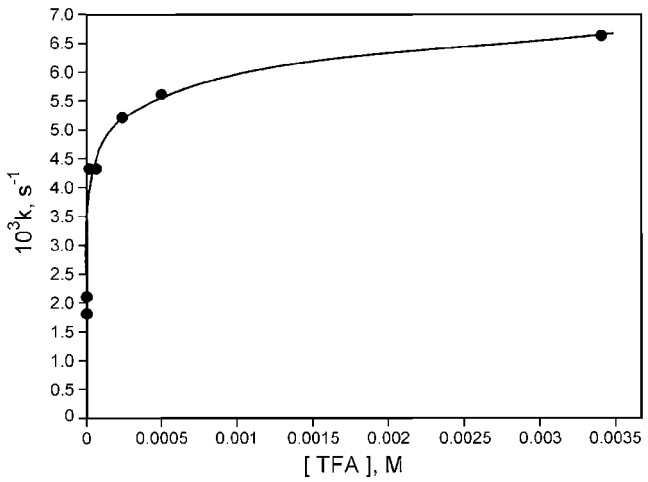

FIGURE 7. Effect of the [TFA] on the racemization rate of **3**.

The 4.3 kcal mol^{-1} lower enantiomerization barrier for the enol **3** than for the acetate **4** seems too high to be ascribed to steric or electronic differences between the OH and OAc groups. We therefore exclude the ββ′-2-ring flip for **3** and suggest that another mechanism which is associated with the presence of the OH group is operating for **3**. To probe this suggestion, the effects of addition of trifluoroacetic acid (TFA), triethylamine (TEA) and the deuterated solvent (98:1:1 hexane: EtOD: *i*-PrOH) were studied.

On raising the concentration of added TFA from 0 to 3.4 × 10^{-3}M, the racemization rate constant increases slightly but systematically from 1.1 × 10^{-3}s^{-1} to 6.6 × 10^{-3}s^{-1} with a sharper increase at lower concentrations (Figure 7). Pronounced curvature of the first-order logarithmic plots was observed at 0.2−2.7 × 10^{-5} M TFA.

The effect of added TEA was complex (Figure 8). At 1.8 × 10^{-5} to 1.8 × 10^{-4}M TEA, the racemization rate increased slightly, but the first order logarithmic plots exhibited curvature that increased with the TEA concentration. At higher [TEA], the rate started to decrease, nearly reaching the "uncatalyzed" rate at 9 × 10^{-4} M, and the plots became linear. At still higher [TEA], the racemization rate drops further, and at 9 × 10^{-3} M TEA, it was sufficiently slow to enable the collection of a small amount of the pure enantiomers and the recording of their CD spectra (Figure 9).

On replacing in the 98:1:1 hexane: EtOH: *i*-PrOH solvent the EtOH by EtOD, the rate was reduced 1.5-fold. Due to proton exchange between the protic solvents and the enol, the effect is due to a combination of solvent isotope effect and a primary isotope effect.

The racemization of **4** was unaffected by TFA, TEA, or EtOD.

Mechanism. There is a mechanistic difference between the racemization of enol **3** and its acetate **4**.

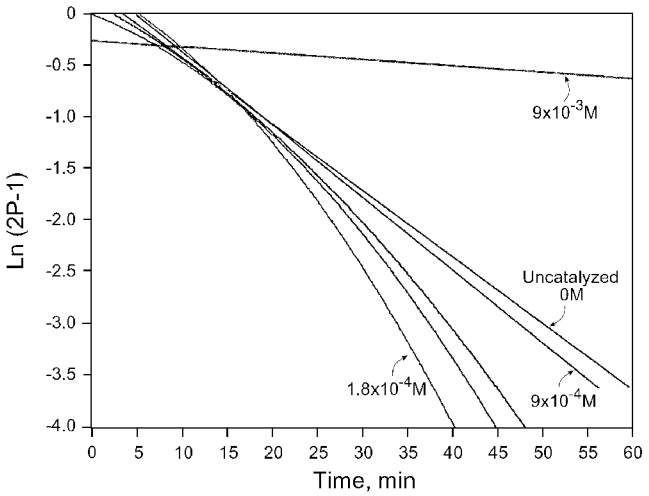

FIGURE 8. Effect of the [TEA] on the racemization rate and the shape of the first order plots of ln(2P-1) vs time for **3**.

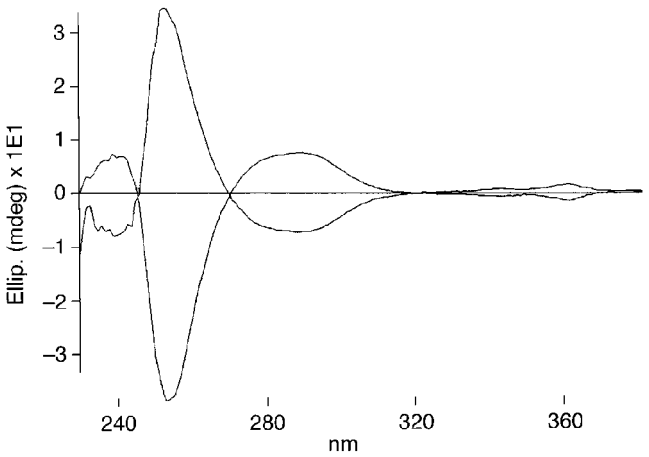

FIGURE 9. CD spectra for the two resolved enantiomers of **3**.

Whereas **4** racemizes via the expected $\beta\beta'$-2-ring flip route which was observed earlier for the enantiomerization of 1-(*m*-methoxymesityl)-2,2-dimesitylvinyl acetate[7] and 1-(*m*-methoxymesityl)-2,2-dimesitylvinyl isopropyl ether,[5] **3** does not enantiomerize via the $\beta\beta'$-2-ring flip route and the following evidence indicates the operation of a new route. (a) A discrepancy between the data obtained by DNMR or by the kinetics of the racemization. From the analysis of possible flip processes for **3** and from the observation by DNMR of two different barriers for the β- and β'-rings, we deduce that the $\beta\beta'$-2-ring flip barrier should be the higher of these two values or higher than both. However, the barrier measured by the kinetics is lower than both values, excluding this route as the threshold enantiomerization for **3**.[15] (b) The observation of acid catalysis, nonlinear base catalysis and solvent isotope effect are inconsistent with a ring-flip process in **3** and with the absence of catalysis for triarylvinyl-X system with X ≠ OH, including the closely related acetate **4**. (c) The enantiomerization barrier for **4** with proper parameters for a flip process is significantly higher than that for **3**.

It is likely that the new route is due to the presence of the vinylic OH group in **3** and (see b above) involves protonation and deprotonation step(s). A corroboration for this and for the mechanism suggested below is the close similarity between the racemization of **3** and the E/Z isomerization of triarylethenol **17**.[9] Such isomerization is exclusive for triarylethenols **1**, X = OH, and not observed when X ≠ OH. We therefore assume that both racemization and E/Z isomerization proceed via the same type of intermediate, where the rotation around the C1−Ar and C1−C2 bonds is more facile than that in the neutral enol.

The five nonflip processes mentioned in the Introduction section accompanied by rings rotation should be considered as possible routes for the enantiomerization of the enols (Figure 3). (i) A simple internal rotation around the C=C bond leads only to topomerization and only if it is accompanied by the rotation of the rings, it may result in enantiomerization. However, this route is excluded since rotation around the C=C bond should have a high barrier as judged by the calculated force field $\Delta H^{\neq}$ values of 51.7 and 39.8 kcal mol^{-1} for such rotation in trimesitylethenol and its enolate ion, respectively.[9] Moreover, this route does not explain the effects of TEA and TFA.

(ii) Ketonization−rotation−enolization is unique to the enols and rotations of the rings and around the C1−C2 bond found in the ketone are less restricted than in the enol.[16] However, this route is inconsistent with the much slower ketonization of such sterically crowded enols than our racemization. For example, the structurally related trimesitylethenol does not ketonize spontaneously and TFA catalyzed ketonization to an equilibrium mixture containing 1.2% of trimesitylethanone took >48 h at 353.6 K.[16] Moreover, whereas the DNMR study displayed two processes with different $\Delta G^{\ddagger}$s for the exchange of the diastereotopic sites of the β and β' rings (Table 5), the β and β' rings in 1,2,2-trimesitylethanone display identical chemical shifts and degenerate processes with $\Delta G^{\ddagger}$<9.5 kcal mol^{-1} exchange their sites.[16] The same applies in our case.

(iii) Protonation on the OH group followed by C−OH_2^+ heterolysis to form a linear vinyl cation which is captured by H_2O from both sides of the empty orbital is excluded for several reasons: (a) There is no precedent for vinyl cation formation by such a route and the rate of the ion formation is likely to be slower than the observed racemization rate.[17] (b) This route should not be catalyzed by TEA. (c) An equilibrium protonation of the OH should be much faster than the C−OH_2^+ heterolysis and an inverse solvent isotopic effect $k_{ROH}/k_{ROD} < 1$ is expected, whereas the observed value is 1.5. (d) If such a route applies for enol **3**, the enol acetate **4** with its better AcO nucleofuge should react in the presence of TFA at least as fast as **3**, contrary to observation. (e) The β- and β'-rings are less sterically hindered in the sp-vinyl cation than in the sp^2-**3**. Due to their equivalence they should display equal barriers for the edges exchange, contrary to observation.

(15) The enantiomerization barrier by kinetics and the DNMR β'-Mes-H exchange barrier (21.9 and 24.6 kcal mol^{-1}, respectively) were measured at 298.5 and 446.6 K, respectively. The assumption that both measure the same process leads to a $\Delta S_e^{\ddagger} = -18.5$ eu which is inconsistent with a monomolecular ring-flip process.

(16) Biali, S. E.; Rappoport, Z. *J. Am. Chem. Soc.* **1985**, *107*, 1007.

(17) Stang, P. J.; Rappoport, Z.; Hanack, M.; Subramanian, L. R. *Vinyl Cations*, Academic Press: New York, 1979; Rappoport, Z.; Stang, P. J. *Dicoordinated Carbocations*, Wiley: Chichester, 1997.

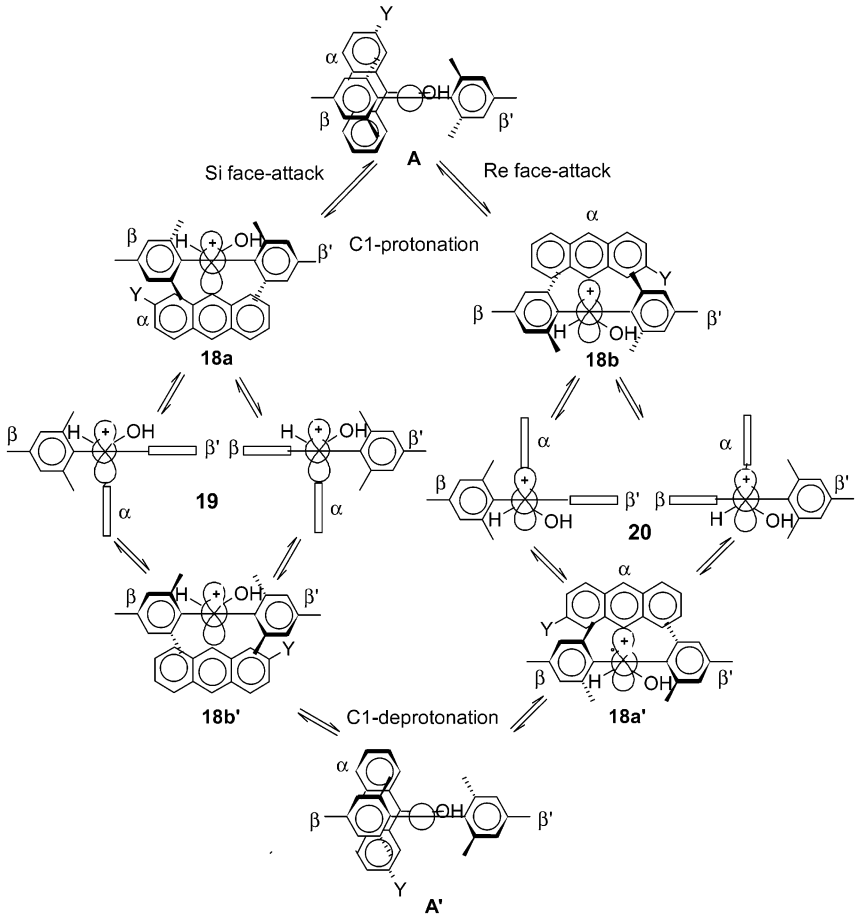

FIGURE 10. Possible enantiomerization route for **3** via the C1-protonated carbenium ions **18a** and **18b**.

(iv) C=C bond protonation at C2, followed by rings and C1−C2 bond rotation is excluded for the reasons given in (ii) above because it is a rate determining step in the acid-catalyzed ketonization, and the β- and β'-rings in the cation are likely to be equivalent.

However, route (v), which involves protonation of the less sterically hindered C1, could be faster than protonation on C2.[18] The carbenium ions **18a** and **18b** (Figure 10), formed by protonation at the diastereotopic faces of the double bond of **3**, have nonequivalent β and β' rings, especially when the rotation rate around the C1−C2 bond is comparable with or slower than that of the rings. The two mesityl rings at the sp^2-C2 are expected to adopt a propeller conformation.

For an enantiomerization to occur, the 1-anthryl ring in **18a** and **18b** must rotate and pass through the plane perpendicular to the $HC9_{(Ant)}O$ plane as in the transition states **19** and **20**. It is conceivable that one of the two processes responsible for the β- and β'-Mes edges exchange observed by DNMR is associated with the observed racemization process. This assumption requires an independent corroboration because it is unclear if the β- and β'-ring rotations in **18a** and **18b** are correlated with the anthryl group motion and if the energies of the respective transition states will be lower than those for the $\alpha\beta'$- and the $\alpha\beta$-2-ring flips in **3**.

We note that except for the argument against route (iv) brought above, the other data are consistent with either C1 or C2 protonation. This mechanism is preferred, since it is consistent with all the experimental data and is therefore discussed. First, the very moderate TFA catalysis could be ascribed to a very slightly higher (by ca. 1 kcal mol^{-1}) $\Delta G^{\ddagger}$ for the proton transfer **3** ⇌ **18** than for the internal rotation in the cation via transition state **19** or **20**. In the absence of TFA, protonation by another enol molecule takes place. Small amounts of added TFA first increase the rate sharply (Figure 7), but on further addition of TFA, the protonation rate becomes first equal and then exceed the internal rotation rate, thus moderating the rate increase.

Second, the complex catalytic effect of TEA (Figure 8) resembles that found for the E/Z-isomerization of **17** which displayed a bell shape curve for the catalysis by pyridine, moderate kinetic isotope effect, self-catalysis by

(18) From solvolysis data of α-Mes and α-9-Ant systems leading to sp^2-hybridized (Charlton, C.; Hughes, E. D. *J. Chem. Soc.* **1956**, 850; Shieh, N. Ph.D. Thesis, 1957. Bryn Mawr College) and sp-hybridized (Rappoport, Z.; Shulman, P,; Thuval (Shoolman) M. *J. Am. Chem. Soc.* **1978**, *100*, 7041) it can be deduced that the stabilities of the transition states leading to planar α-9-anthrylalkyl and α-mesitylalkyl cations are roughly the same. Ar-substituted cations with propeller conformations (e.g., Ar_3C^+) are appreciably stabilized and the solvolysis of precursors to diarylalkyl cations was analyzed in terms of the propeller conformation (Fujio, M.; Kim, H.-J.; Uddin, M. K.; Yoh, S.-D.; Rappoport, Z.; Tsuno, Y. *J. Phys. Org. Chem.* **2002**, *15*, 330). We calculated that dimesitylalkyl cation with Mes-C^+ dihedral angles close to those in **4** is approximately as stabilized as a planar Mes-C^+ ion. Hence, neglecting other effects, C1 protonation, leading to **18**, and C2 protonation have close probabilities. It is difficult to evaluate the contributions of the combined additional stabilization by the OH and destabilization by the 2-F in the C2 protonated ion, the different electron withdrawal by the β-groups in both cations and the lower steric effect to protonation at C1 than at C2, and the only conclusion is that protonation at C1 is a viable possibility, especially in view of the argument brought above against C2 protonation.

SCHEME 2. Third Order Term in the Enol for the E/Z Isomerization of 17 as a Possible Explanation of Base Catalysis at Low Base Concentrations

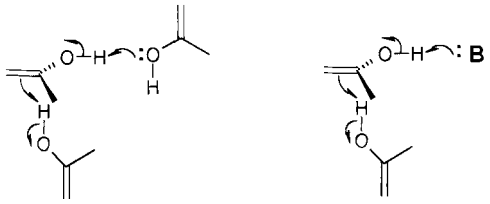

the enol, and a barrier of 22.4 kcal mol^{-1} in $CDCl_3$.[9] The pseudo-first-order rate constant (= rate/[enol]) for this reaction display a quadratic curved dependence on the [enol], suggesting a competition between routes that involve second and third-order term in the enol.[19] A similar explanation applies in the case of **3**. The third-order term may be ascribed to a concerted step[20] (or two consecutive steps with close $\Delta G^{\ddagger}$s) when one enol molecule serves as a proton donor and the other as a proton acceptor for the racemizing enol (Scheme 2). When the latter is replaced by a stronger base (pyridine, TEA) catalysis will take place at low base concentration. At a higher base concentration, the concentration of the protonated enol is reduced with a consequent inhibition of the racemization.

Third, the low value of the solvent isotope effect for the racemization of **3** in the organic medium is partially due to the fact that in the labeled solvent the ROD consists only 57% of the ROH + ROD mixture.[21] It is consistent with a partial rate determining hydrogen transfer and should be regarded only qualitatively as a $k_{ROH}/k_{ROD} > 1$.

This mechanism is regarded as tentative and requires an additional corroboration. For **2**, whose DNMR behavior and racemization were qualitatively similar to those of **3**, we assume a similar mechanism.

Conclusions

Stereoisomerizations of sterically crowded 1-[9′-(2′-Yanthryl)]-2,2-dimesitylethenols (**2**,**3**) and acetate (**4**) were studied by DNMR and that of **3** and **4** also by chiral HPLC method. These compounds undergo rotational threshold 3-ring flip diastereomerization with $\Delta G^{\ddagger}$s of 15.7, 16.6, and 16.6 kcal mol^{-1}, respectively, but the enantiomerization routes differ for **3** and **4**. Acetate **4** was resolved to its enantiomers and it most likely enantiomerizes by a rotational $\beta\beta'$-2-ring flip with $\Delta G_{\beta\beta'}^{\ddagger} = 26.2$ kcal mol^{-1}, $\Delta S_{\beta\beta'}^{\ddagger} = 4.3$ eu which is insensitive to mild concentrations of added acids and bases. The enantiomerization of **3** proceeds by a different, much faster process, which is affected by added TFA or TEA and display a solvent isotope effect > 1 in 98:1:1 hexane: EtOH: *i*-PrOH. Resolution of **3** to its enantiomers and their isolation was achieved only after inhibiting the racemization by TEA. Examination of various isomerization routes revealed that a route involving C1-protonation of the enolic double bond is consistent with all the experimental data. It is unclear if rotation of the rings in the intermediate carbocation is correlated and if it is responsible for the β- and β'-rings edge exchange observed in the DNMR experiment.

Experimental Section

General Methods, Solvents, and Materials. Melting points, ^{1}H NMR and ^{19}F NMR spectra were determined according to the literature.[8,22] Proton assignments were based in several cases on COSY and NOESY methods. HPLC chiral resolutions and subsequent kinetic measurements were performed using an amylose tris(3,5-dimethylphenylcarbamate) coated on 10 μm silica gel column[23] and detection was at 280 and 400 nm. The mobile phase was a 99:1 or 98:2 hexane: *i*-PrOH for **2** and **3** and 80:20 hexane: *i*-PrOH for **4**. Solvents and materials were purified and purchased as previously described.[22]

2-Hydroxyanthraquinone (9). To a solution of commercial 2-aminoanthraquinone (10 g, 45 mmol; **Warning! Highly carcinogenic!**) in 96% H_2SO_4 (130 mL) at 0 °C $NaNO_2$ (3.8 g, 55 mmol) was added portionwise with stirring. The solution was stirred for 3.5 h at room temperature and then poured into ice (500 g). The resulting solution of diazonium hydrogen sulfate was refluxed for 30 min during which a greenish-yellow precipitate was formed. After cooling to room temperature, the solid was filtered, washed with water and air-dried. Crystallization from glacial AcOH gave 9.64 g (96%) of **9** as yellow needles, mp 301 °C (lit:[24] 302−303 °C).

2-Anthraquinone Diazonium Tetrafluoroborate (10). When the cold (0 °C) solution of the diazonium hydrogen sulfate, which was prepared as described for **9**, was poured into an aqueous solution (150 mL) of $NaBF_4$ (6.8 g, 62 mmol) at 0 °C, a greenish-gray precipitate was formed. The mixture was stirred for an additional 1 h, the precipitate was filtered; washed consecutively with cold water, cold methanol, and ether, and dried at room temperature, giving 12.1 g (83%) of crude **10**, which was used without further purification.

2-Fluoroanthraquinone (11). The crude salt **10** (12 g, 37.3 mmol) was thermally decomposed according to a standart procedure for aromatic diazonium fluoroborates.[25] Sublimation of the crude product gave **11** (3.62 g, 43%) as bright yellow crystals, mp 204 °C (lit:[26] 204 °C). ^{1}H NMR ($CDCl_3$) δ (ppm): 7.47 (1H, ddd, $^3J_{HH} = 8.3$ Hz, $^3J_{HF} = 8.3$ Hz, $^4J_{HH} = 2.7$ Hz), 7.83 (2H, m), 7.95 (1H, dd, $^3J_{HF} = 8.7$ Hz, $^4J_{HH} = 2.7$ Hz), 8.32 (2H, m), 8.37 (1H, dd, $^3J_{HH} = 8.7$ Hz, $^4J_{HF} = 5.3$ Hz).

2-Hydroxyanthracene (12). 12 was prepared according to the literature procedure.[11] Column chromatography of the crude product on silica gel using CH_2Cl_2 eluent gave **12** as a first fraction (2.32 g, 31%), which was used without further purification. ^{1}H NMR (CD_3CN) δ (ppm): 7.17 (1H, dd, ^3J = 9.1 Hz, ^4J = 2.4 Hz), 7.27 (1H, d,^4J = 2.2 Hz), 7.43 (2H, m), 7.97 (2H, 2d, ^3J = 8.2 Hz), 7.97 (1H, d, ^3J = 9.0 Hz), 8.27, 8.41 (2H, 2s). ν_{max}(Nujol): 3500, 3210−3220 (OH) cm^{-1}, 1640 (C=C) cm^{-1}.

Other fractions contained the precursor **9**, 2-hydroxyanthrone and 2,9,10-trihydroxy-9,10-dihydroanthracene according to TLC and NMR spectra.

2-Acetoxyanthracene (14). A solution of **12** (2.10 g, 10.8 mmol) in pyridine (20 mL)-Ac_2O (6 mL) was refluxed for 2 h and then poured into cold water (250 mL) giving a white milky

(19) Bunnett, J. F. In *Investigation of Rates and Mechanisms of Reactions*, 4th ed.; Bernasconi, C. F., Ed., Wiley: Chichester, 1986; Chapter 4, p 282.

(20) Keeffe J. R.; Kresge, A. J. In *The Chemistry of Enols*; Rappoport, Z. Ed., Wiley: Chichester, 1990; Chapter 7, pp 434−446.

(21) Saunders, W. H., Jr. In *Investigation of Rates and Mechanisms of Reactions*, 4th ed.; Bernasconi, C. F., Ed., Wiley: Chichester, 1986; Chapter 8, pp 601−604.

(22) (a) Frey, J.; Rappoport, Z. *J. Org. Chem.* **1997**, *62*, 8372. (b) Lei, Y. X.; Cerioni, G.; Rappoport, Z. *J. Org. Chem.* **2001**, *66*, 8379.

(23) Okamoto, Y.; Kaida, Y.; Hayashida, H.; Hatada, K. *Chem. Lett.* **1990**, 909.

(24) Mihai, G. G.; Tarassoff, P. G., Filipescu, N. *J. Chem. Soc., Perkin Trans. 1* **1975**, 1374.

(25) *Vogel's Textbook of Practical Organic Chemistry*, 5th ed.; Longman: New York, 1989; pp 939−941.

(26) Meyer, A. Y.; Goldblum, A. *Isr. J. Chem.* **1973**, *11*, 791.

suspension. The mixture was acidified with HCl to pH 3−4, stirred for additional 1h and the precipitate formed was filtered, washed twice with cold water and air-dried. Recrystallization from EtOH gave **14** (2.18 g, 85%) as a white powder, mp 198 °C (lit:[12] 198 °C); ^{1}H NMR ($CDCl_3$) δ (ppm): 2.38 (3H, s), 7.23 (1H, dd, ^3J = 9.1 Hz, ^4J = 2.2 Hz), 7.47 (2H, m), 7.71 (1H, d, ^4J = 1.8 Hz), 7.99 (2H, 2d, ^3J = 8.6 Hz), 8.02 (1H, d, ^3J = 9.0 Hz), 8.37, 8.43 (2H, 2s). ν_{max} (Nujol): 1760 (C═O), 1640 (C═C) cm^{-1}.

2-Fluoroanthracene (13). A solution of **11** (2.5 g, 11 mmol) in AcOH (100 mL) was refluxed with 57% HI (11 mL) for 60 h. The mixture was cooled to room temperature and poured into water (300 mL). The precipitate that formed was filtered and dried. According to ^{1}H NMR, it is a 7:3 mixture of **13** to 2-fluoro-9,10-dihydroanthracene. A small excess of iodine (0.88 g, 3.5 mmol) was added to the solid in refluxing toluene (150 mL) until the 9,10-dihydro derivative was disappeared according to TLC. The mixture was cooled to room temperature, washed successively with 5% $NaHCO_3$ (150 mL), saturated $Na_2S_2O_3$ solution (150 mL) and water (150 mL) and evaporated to dryness under reduced pressure. The yellow residue was recrystallized from AcOH giving **13** (1.85 g, 86%) as off-white crystals, mp 212 °C (lit:[26] 212 °C); ^{1}H NMR ($CDCl_3$) δ (ppm): 7.27 (1H, ddd, $^3J_{HH} = {}^3J_{HF}$ = 8.9 Hz, $^4J_{HH}$ = 2.5 Hz), 7.47 (2H, m,), 7.57 (1H, dd, $^3J_{HF}$ = 10.2 Hz, $^4J_{HH}$ = 2.4 Hz), 7.99 (3H, m), 8.35, 8.43 (2H, 2s).

2-Acetoxy-9-bromoanthracene (15). A solution of 2-acetoxyanthracene **14** (1.7 g, 7.2 mmol) in hot AcOH (50 mL) was cooled rapidly to 20 °C. To the suspension thus formed, a solution of bromine (0.85 mL, 16.5 mmol) in AcOH (15 mL) was added slowly over 1.5 h. The reaction was monitored by TLC using 2:1 $CHCl_3$:petroleum ether eluent (R_f: **14**, 0.15; **15**, 0.75; 9,10-dibromo derivative, 0.9). The addition of bromine was stopped when only a small amount of **14** had remained in the mixture but accumulation of the dibromo derivative was still insignificant. The suspension then turned immediately into a clear solution which was poured into water (250 mL). The yellow, fine suspension that was formed was stirred with heating at 60−70 °C for 2 h. The precipitate that formed was filtered, washed thoroughly with water, dried in vacuo, and purified by flash chromatography, giving a mixture of **15** and the 9,10-dibromo derivative (0.09 g) as a first fraction and then 2.1 g of **15**. Recrystallization from AcOH gave pure **15** (1.77 g, 78%) as yellow needles, mp 110 °C. ^{1}H NMR ($CDCl_3$) δ (ppm): 2.41 (3H, s, CH_3), 7.28 (dd, H_3 partly overlaps the $CHCl_3$ signal), 7.50, 7.62 (2H, 2m, H_6,H_7), 7.99 (1H, d, ^3J = 7.7 Hz, H_5), 8.02 (1H, d, ^3J = 9.1 Hz, H_4), 8.22 (1H, d, ^4J = 2 Hz, H_1), 8.44 (1H, s, H_{10}), 8.48 (1H, d, ^3J = 8.9 Hz, H_8). Anal. Calcd for $C_{16}H_{11}BrO_2$: C, 60.98; H, 3.52; Found: C, 61.19; H, 3.47%.

9,10-Dibromo-2-acetoxyanthracene. ^{1}H NMR ($CDCl_3$) δ (ppm): 2.42 (3H, s, CH_3), 7.40 (1H, dd, ^3J = 9.5 Hz, ^4J = 2.2 Hz, H_3), 7.64 (2H, m, H_6,H_7), 8.31 (1H, d, ^4J = 2.2 Hz,H_1), 8.56 (2H, m, H_5,H_8), 8.63 (1H, d, ^3J = 9.5 Hz, H_4).

9-Bromo-2-methoxyanthracene (5). A suspension of **15** (1.77 g, 5.6 mmol) in 5% aqueous NaOH (50 mL) was stirred at 50−60 °C for 20 min, until a greenish-yellow fluorescent solution was formed. The solution was cooled to room temperature, dimethyl sulfate (1 mL) was added, stirring continued for about 8−10 h and the orange precipitate which was gradually formed was filtered, washed with water and recrystallized from EtOH, yielding pure **5** (1.32 g, 82%) as orange crystals, mp 116 °C. ^{1}H NMR ($CDCl_3$) δ (ppm): 4.02 (3H, s, OCH_3), 7.17 (1H, dd, ^3J = 9.1 Hz, ^4J = 2.3 Hz, H_3), 7.43 (1H, m, H_6), 7.57 (1H, m, H_7), 7.66 (1H, bs, H_1), 7.86 (1H, d, ^3J = 9.1 Hz, H_4), 7.94 (1H, d, ^3J = 8.4 Hz, H_5), 8.32 (1H, s, H_{10}), 8.44 (1H, d, ^3J = 8.9 Hz, H_8). Anal. Calcd for $C_{15}H_{11}BrO$: C, 62.74; H, 3.86; Found: C, 62.51; H, 3.99%.

9-Bromo-2-fluoroanthracene (6). 13 (1.17 g, 6 mmol) was brominated by a procedure similar to that described for **15**, yielding after chromatography and crystallization from AcOH 1.15 g (70%) of **14** as yellow crystals, mp 118−119 °C. ^{1}H NMR ($CDCl_3$) δ (ppm): 7.31 (1H, ddd, $^3J_{HH}$ = 7.8 Hz, $^3J_{HF}$ = 9.4 Hz, $^4J_{HH}$ = 2.4 Hz, H_3), 7.51 (1H, m, H_6), 7.63 (1H, m, H_7), 8.00 (1H, d, $^3J_{HH}$ = 8.2 Hz, H_5), 8.02 (1H, dd, $^3J_{HH}$ = 9.2 Hz, $^4J_{HF}$ = 5.9 Hz, H_4), 8.13 (1H, dd, $^3J_{HF}$ = 11.5 Hz, $^4J_{HH}$ = 2.4 Hz, H_1), 8.45 (1H, s, H_{10}), 8.47 (1H, d, $^3J_{HH}$ = 9.0 Hz, H_8). Anal. Calcd for $C_{14}H_8BrF$: C, 61.12; H, 2.93; Found: C, 61.28; H, 2.99%.

9,10-Dibromo-2-fluoroanthracene. mp 205−206 °C (from EtOH); ^{1}H NMR ($CDCl_3$) δ (ppm): 7.41 (1H, ddd, $^3J_{HH}$ = 9.7 Hz, $^3J_{HF}$ = 9.4 Hz, $^4J_{HH}$ = 2.4 Hz, H_3), 7.63 (2H, m, H_6,H_7), 8.20 (1H, dd, $^3J_{HF}$ = 11.0 Hz, $^4J_{HH}$ = 2.5 Hz, H_1), 8.53 (2H, m, H_5, H_8), 8.61 (1H, dd, $^3J_{HH}$ = 9.7 Hz, $^4J_{HF}$ = 5.9 Hz, H_4). Anal. Calcd for $C_{14}H_7Br_2F$: C, 47.50; H, 1.99; Found: C, 47.74; H, 1.94%.

1-[9′-(2′-Methoxyanthryl)]-2,2-dimesitylethenol (2). To a solution of **5** (1.0 g, 3.5 mmol) in dry ether (20 mL), 2.5 M BuLi in hexane (1.5 mL, 3.75 mmol) was added at 0 °C. The mixture was stirred for 30 min at 0 °C, and a solution of dimesitylketene[10] (1.0 g, 3.6 mmol) in dry THF (40 mL) was added over 15 min. The mixture was refluxed overnight, poured into ice (200 g)/concentrated HCl (10 mL), extracted with chloroform (3 × 50 mL) and the combined organic phase was dried ($MgSO_4$) and evaporated. The residue was purified by column chromatography on silica gel using consecutively petroleum ether and 70:30 petroleum ether − chloroform as the eluents, giving **2** (525 mg, 31%) as an orange solid (^{1}H NMR data given in Table 3). An analytical sample was crystallized from 2-propanol giving the 1:1 adduct **2**·*i*-PrOH as orange crystals, mp 104 °C (dec). Anal. Calcd for $C_{38}H_{42}O_3$: C, 83.48; H, 7.74. Found: C, 83.76; H, 7.59%.

1-[9′-(2′-Fluoroanthryl)]-2,2-dimesitylethenol (3). The enol was prepared as described above for **2** from **6** (1.05 g, 3.8 mmol), 2.5M BuLi (1.5 mL, 3.8 mmol) and dimesitylketene (1.09 g, 3.9 mmol). 635 mg (35%) of a yellow solid were obtained. The sample used in the experiments was crystallized from 2-propanol giving the 1:1 adduct **3**·*i*-PrOH as yellow crystals, mp 136 °C (dec). ^{1}H and ^{19}F NMR data are in Table 3. Anal. Calcd for $C_{37}H_{39}FO_2$: C, 83.11; H, 7.35. Found: C, 83.41; H, 7.27%.

1-[9′-(2′-Fluoroanthryl)]-2,2-dimesitylvinyl Acetate (4). A solution of **3** (300 mg, 0.6 mmol) in pyridine (10 mL)−Ac_2O (3 mL) was refluxed for 2 h and then poured into cold water (100 mL). The mixture was acidified with HCl to pH 3−4, extracted with ether (3 × 50 mL) and the combined organic layer was dried ($MgSO_4$) and evaporated. Crystallization of the solid residue from petroleum ether yielded 251 mg (81%) of **4**, mp 194 °C. The ^{1}H NMR spectrum is in Table 3. Anal. Calcd for $C_{36}H_{33}FO_2$: C, 83.69; H, 6.44. Found: C, 83.94; H, 6.28%.

Crystallographic Parameters of 4. The material crystallized in the *C*2/*c* space group with eight molecules in a cell of dimensions a = 33.431 Å, b = 11.286 Å, c = 15.600 Å, β = 107.05° and V = 5627 Å^3. ρ_{calcd} = 1.22 g cm^{-3}, μ(Mo Kα) = 0.73 cm^{-1}, no. of unique reflections = 4160, no. of reflections with $I \geqslant 2\sigma_I$ = 2629. R = 0.070, R_w = 0.082.

Acknowledgment. We are indebted to Prof. Silvio E. Biali for helpful suggestions and discussions, to Dr. Shmuel Cohen for the crystallographic determination, to Dr. Shulamith Levin for help with the chiral separation and to the Israel Science Foundation for support.

Supporting Information Available: Figure S1 of the stereoview and Tables S1−5 of the details of the crystallographic technique, of bond lengths and angles and of position and thermal parameters of **4**. This material is available free of charge via the Internet at http://pubs.acs.org.

JO020497Q